# Single-Layer Microstrip High-Directivity Coupled-Line Coupler With Tight Coupling

Yongle Wu, Weinong Sun, Sai-Wing Leung, *Senior Member, IEEE*, Yinliang Diao, *Student Member, IEEE*, Kwok-Hung Chan, *Member, IEEE*, and Yun-Ming Siu

***Abstract*—A novel symmetrical coupled-line circuit structure without patterned ground plane is proposed to design tight-coupling high-directivity couplers, which would be found in numerous applications in a microstrip RF front end because of its simple structure and inherent excellent compatibility. Based on a traditional even- and odd-mode technique, closed-form mathematical equations for both circuit electrical parameters and scattering parameters are obtained. Due to the use of two coupled-line sections placed in the vertical direction, the directivity of this novel coupler without any other compensation techniques can be enhanced while maintaining tight-coupling performance of almost 3 dB. For demonstrative purposes, three typical full-wave simulation examples with realized physical dimensions in microstrip technology are presented, indicating high directivity and tight coupling coefficient. Finally, a practical microstrip coupled-line coupler is designed and fabricated to operate at approximately 2 GHz. The measured results show good return loss, quadrature phase characteristics, high directivity, and strong coupling performances.**

***Index Terms*—Coupled line, high directivity, microstrip coupler, tight coupling.**

## I. Introduction

MICROSTRIP coupled-line couplers [1] are widely used for the designs of various balanced power amplifiers, mixers, modulators, measurement systems, circularly polarized antennas, beam-forming array antennas, etc. In practical applications, on the one hand, the coupling level of microstrip coupled-line coupler is mainly limited by the narrow separation between two parallel edge-coupled transmission lines, usually $>0.1$ mm, in the printed circuit board (PCB) fabrication. On the other hand, the poor directivity is mainly due to the difference in the phase velocities of even and odd modes on coupled microstrip lines. In general, only the traditional microstrip quarter-wavelength coupled-line coupler can provide coupling in the 8–40-dB range [1] while the measured directivity is usually smaller than 20 dB [2]. Therefore, the main limitations of the traditional coupled-line couplers are low coupling level and poor directivity in microstrip implementation.

To achieve a tight coupling coefficient of $-3$ dB in microstrip coupled-line couplers, several methods have been studied. For instance, Lange type [3], tandem connected form [4], multilayer broadside-coupled or single-layer with patterned ground plane structures [5]–[9], vertically installed configuration [10], and additional quarter-wavelength *noncoupled* connecting delay lines [11]–[14]. Although these methods can enhance the coupling performance, they may include some disadvantages such as inconvenient extra bonding wires [3], [4], complicated design procedures or multilayer circuitries [5]–[10], and large circuit areas [11]–[14]. It is important that the directivity of these couplers is still poor.

Besides the coupling enhancement approaches, in order to improve the directivity of the microstrip coupled-line couplers, various kinds of compensation techniques have been investigated. These techniques include wiggle-line structure [15], velocities-compensation capacitors [16], [17] or inductors [2], additional output-ports matching networks [18], [19], and a combination of a regular microstrip and a negative-refractive-index line [20]. These techniques can achieve high directivity; however, the coupling coefficients are small. Recently, a novel dual-band coupled-line coupler is proposed in [21]. Note that the low coupling coefficient still exists and the directivity has space for improvement in practical applications.

In this paper, by combining two coupled-line sections, which are different from the *noncoupled* connecting delay lines [11]–[14], a novel coupled-line coupler with tight coupling coefficient and high-directivity performance is proposed, and this is suitable for microstrip PCB realization. Although all coupled lines in this proposed coupler are realized by loosely coupled microstrip structures, they can provide flexible parameters to enhance the coupling capability and compensate the difference between the phase velocities of the even and odd modes, simultaneously. This proposed microstrip coupled-line coupler offers several advantages that include: 1) tight coupling coefficients of almost $-3$ dB; 2) excellent full-wave simulated directivity higher than 60 dB; 3) without any via-holes or wire bonding; 4) easy realization in common microstrip technology with planar loosely coupled structure; 5) analytical design

Manuscript received July 16, 2012; revised December 04, 2012 and December 11, 2012; accepted December 12, 2012. Date of publication January 08, 2013; date of current version February 01, 2013. This work was supported by the RGC-General Research Fund Project 9041680 (CityU 120811) under a grant. This work was supported in part by the National Natural Science Foundation of China (61201027), the Fundamental Research Funds for the Central Universities (2012RC0301 and 2012TX02), Open Project of the State Key Laboratory of Millimeter Waves under Grant K201316, and the Beijing Key Laboratory of Work Safety Intelligent Monitoring, Beijing University of Posts and Telecommunications.

Y. Wu is with the School of Electronic Engineering, Beijing University of Posts and Telecommunications, 100876 Beijing, China, and also with the Department of Electronic Engineering, City University of Hong Kong, Hong Kong, and the State Key Laboratory of Millimeter Waves, Southeast University, Nanjing 210096, China (e-mail: wuyongle138@gmail.com).

W. Sun, S.-W. Leung, Y. Diao, K.-H. Chan, and Y.-M. Siu are with the Department of Electronic Engineering, City University of Hong Kong, Hong Kong.

Color versions of one or more of the figures in this paper are available online at http://ieeexplore.ieee.org.

Digital Object Identifier 10.1109/TMTT.2012.2235855

0018-9480/$31.00 © 2013 IEEE

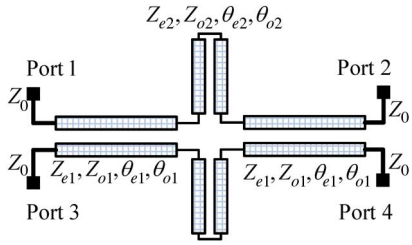


Fig. 1. Original circuit schematic of the proposed compact coupled-line coupler with tight coupling coefficient and high directivity.

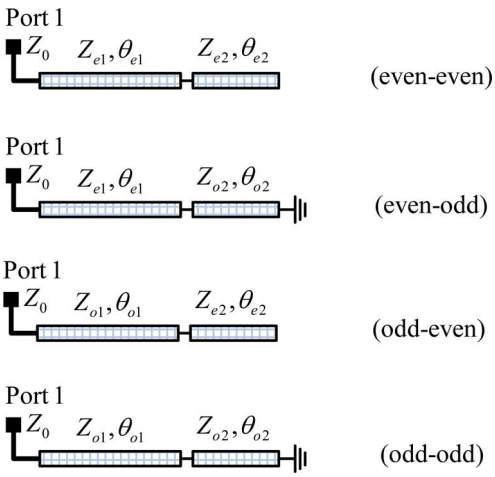


Fig. 2. Equivalent circuit configurations of the proposed coupler under the even and odd symmetric excitations.

equations for initial circuit electrical parameters and scattering parameters; and 6) symmetrical structure in a single layer with intact ground plane.

## II. New Circuit of the Proposed Coupled-Line Coupler and Its Design Theory

Fig. 1 shows the circuit configuration of the proposed coupled-line coupler, which has the advantage of single-layer construct without any patterned ground planes and bond wires. This coupler essentially includes two groups of coupled-line sections. The even-mode characteristic impedance of the first (second) section coupled line is $Z_{e1}(Z_{e2})$, and the odd-mode characteristic impedance of the first (second) section coupled line is $Z_{o1}(Z_{o2})$. Without loss of generality, the even- and odd-mode electrical lengths at the operating frequency of the first (second) section coupled line are $\theta_{e1}(\theta_{e2})$ and $\theta_{o1}(\theta_{o2})$, respectively. In addition, the port impedance is defined as $Z_0$.

Since the proposed structure shown in Fig. 1 has inherent symmetry, for simplification, the even–odd decomposition method described in [22] and [23] is applied to analyze the whole coupled-line coupler structure. This structure has twofold symmetry along the horizontal and vertical directions. It is very simple that the four-port structure depicted in Fig. 1 is simplified as four one-port structures shown in Fig. 2.

The scattering parameters of the proposed coupled-line coupler can be expressed in terms of its corresponding single-port circuits, which is given by [22], [23]

$$S_{11} = \frac{\Gamma_{ee} + \Gamma_{eo} + \Gamma_{oe} + \Gamma_{oo}}{4} \tag{1a}$$

$$S_{21} = \frac{\Gamma_{ee} - \Gamma_{eo} + \Gamma_{oe} - \Gamma_{oo}}{4} \tag{1b}$$

$$S_{31} = \frac{\Gamma_{ee} + \Gamma_{eo} - \Gamma_{oe} - \Gamma_{oo}}{4} \tag{1c}$$

$$S_{41} = \frac{\Gamma_{ee} - \Gamma_{eo} - \Gamma_{oe} + \Gamma_{oo}}{4}. \tag{1d}$$

Due to the symmetry feature in the planar structure, (1) can completely represent other scattering parameters values of the proposed couple-line coupler. $\Gamma_{ee}$, $\Gamma_{eo}$, $\Gamma_{oe}$, and $\Gamma_{oo}$ are the input reflection coefficients for the even–even-, even–odd-, odd–even-, and odd–odd-mode equivalent circuits, as shown in Fig. 2, respectively.

For mathematical simplification, all characteristic impedance values are normalized with respect to the port impedance $Z_0$, which is expressed as

$$z_{e1} = \frac{Z_{e1}}{Z_0} \quad z_{o1} = \frac{Z_{o1}}{Z_0} \quad z_{e2} = \frac{Z_{e2}}{Z_0} \quad z_{o2} = \frac{Z_{o2}}{Z_0}. \tag{2}$$

Based on the conventional transmission-line theory, the input reflection coefficients can be calculated by

$$\Gamma_{ee} = \frac{z_{inee} - 1}{z_{inee} + 1} \tag{3a}$$

$$\Gamma_{eo} = \frac{z_{ineo} - 1}{z_{ineo} + 1} \tag{3b}$$

$$\Gamma_{oe} = \frac{z_{inoe} - 1}{z_{inoe} + 1} \tag{3c}$$

$$\Gamma_{oo} = \frac{z_{inoo} - 1}{z_{inoo} + 1} \tag{3d}$$

where

$$z_{inee} = jz_{e1}\frac{z_{e1}\tan(\theta_{e1})\tan(\theta_{e2}) - z_{e2}}{z_{e1}\tan(\theta_{e2}) + z_{e2}\tan(\theta_{e1})} \tag{4a}$$

$$z_{ineo} = jz_{e1}\frac{z_{e1}\tan(\theta_{e1}) + z_{o2}\tan(\theta_{o2})}{z_{e1} - z_{o2}\tan(\theta_{e1})\tan(\theta_{o2})} \tag{4b}$$

$$z_{inoe} = jz_{o1}\frac{z_{o1}\tan(\theta_{o1})\tan(\theta_{e2}) - z_{e2}}{z_{o1}\tan(\theta_{e2}) + z_{e2}\tan(\theta_{o1})} \tag{4c}$$

$$z_{inoo} = jz_{o1}\frac{z_{o1}\tan(\theta_{o1}) + z_{o2}\tan(\theta_{o2})}{z_{o1} - z_{o2}\tan(\theta_{o1})\tan(\theta_{o2})}. \tag{4d}$$

If the perfect input-port matching and isolation conditions are satisfied simultaneously, (1a) and (1d) lead to

$$\begin{cases} \Gamma_{ee} + \Gamma_{oo} = 0 \\ \Gamma_{eo} + \Gamma_{oe} = 0. \end{cases} \tag{5}$$

After combining (3) and (5), we can obtain

$$z_{inee}z_{inoo} = z_{ineo}z_{inoe} = 1. \tag{6}$$

If a 90° coupler with arbitrary power division is designed, the relationship of the coupling and transmission parameters should be

$$S_{21} = jkS_{31} \tag{7}$$

where $k$ is the power-dividing coefficient. Similarly, after combining (1), (3), and (7), another important equation can be found as

$$kj(z_{inee}z_{ineo} - 1) = z_{inee} - z_{ineo}. \tag{8}$$

To easily solve these nonlinear equations and achieve compact size applications for this proposed coupler, the following constrains are assumed for the initial design:

$$\begin{cases} \theta_1 = \theta_{e1} = \theta_{o1} \\ \theta_2 = \theta_{e2} = \theta_{o2} \end{cases} \tag{9a}$$

$$\begin{cases} 0 < \theta_1 \leq 90^0 \\ 0 < \theta_2 \leq 90^0. \end{cases} \tag{9b}$$

After condition (9) is considered, two different cases to solving (6) and (8) are solved separately.

Case 1: The condition is $\theta_1 = 90^\circ$.

By substituting (9a) and the condition $\theta_1 = 90^\circ$ into (4), the following four relationships can be obtained:

$$z_{inee} = \frac{jz_{e1}^2 \tan(\theta_2)}{z_{e2}} \tag{10a}$$

$$z_{ineo} = \frac{-jz_{e1}^2}{z_{o2}\tan(\theta_2)} \tag{10b}$$

$$z_{inoe} = \frac{jz_{o1}^2 \tan(\theta_2)}{z_{e2}} \tag{10c}$$

$$z_{inoo} = \frac{-jz_{o1}^2}{z_{o2}\tan(\theta_2)}. \tag{10d}$$

Combining (6), (8), and (10) leads to the following equations:

$$\begin{cases} (z_{e1}z_{1o})^2 = z_{e2}z_{o2} \\ k(z_{e1}^4 - z_{e2}z_{o2})\tan(\theta_2) = z_{e1}^2 z_{o2}\tan^2(\theta_2) + z_{e1}^2 z_{e2}. \end{cases} \tag{11}$$

Notice that there are five unknowns, i.e., $z_{e1}$, $z_{o1}$, $z_{e2}$, $z_{o2}$, and $\theta_2$, but only two conditions of (11) are available. Here, the electrical length $\theta_2$ is assumed as a known parameter. Different known parameter assumptions for normalized characteristic impedances in (11) will result in different analytical solutions. Based on known parameters $z_{e1}$ and $z_{o1}$, the first group of solutions can be given by

$$\begin{cases} z_{e2} = \dfrac{kz_{e1}^2\left(z_{e1}^2 - z_{o1}^2\right) + \sqrt{k^2 z_{e1}^4\left(z_{e1}^2 - z_{o1}^2\right)^2 - 4z_{e1}^6 z_{o1}^2}}{2z_{e1}^2\cot(\theta_2)} \\ z_{o2} = \dfrac{kz_{e1}^2\left(z_{e1}^2 - z_{o1}^2\right) - \sqrt{k^2 z_{e1}^4\left(z_{e1}^2 - z_{o1}^2\right)^2 - 4z_{e1}^6 z_{o1}^2}}{2z_{e1}^2\tan(\theta_2)}. \end{cases} \tag{12}$$

The second group of solutions is based on known parameters $z_{e2}$ and $z_{o2}$, which is (13), shown at the bottom of this page. Since the loose coupling coefficient of the first section coupled line should be predefined manually, solution (12) becomes more useful than solution (13).

Case 2: The condition is $\theta_1 \neq 90^\circ$

In this case, the electrical lengths of two-section coupled lines are not fixed and the solutions are more general. From (4) and (6), we can obtain the following relationship:

$$\begin{cases} z_{e1}z_{o1} = 1 \\ z_{e2}z_{o2} = 1. \end{cases} \tag{14}$$

From (4) and (8), the following condition should be satisfied:

$$\begin{aligned} &kz_{e1}^2\left[z_{e2} - z_{e1}\tan(\theta_1)\tan(\theta_2)\right]\left[z_{e1}\tan(\theta_1) + z_{o2}\tan(\theta_2)\right] \\ &\quad + k\left[z_{e1}\tan(\theta_2) + z_{e2}\tan(\theta_1)\right]\left[z_{o2}\tan(\theta_1)\tan(\theta_2) - z_{e1}\right] \\ &\quad = -(z_{e1})^2\left[1 + \tan^2(\theta_1)\right]\left[z_{e2} + z_{o2}\tan^2(\theta_2)\right] \end{aligned} \tag{15}$$

Equations (14) and (15) can be easily solved when the parameters $z_{e1}, \theta_1$, and $\theta_2$ are assumed as known constant numbers. Mathematically, the solutions for (14) and (15) are shown in (16) at bottom of the following page. Next, let us establish the connection between the (12) and (16). If directly substituting the condition $\theta_1 = 90^\circ$ into the generalized solution

$$\begin{aligned} z_{e1} &= \sqrt{\frac{\sqrt{\left[z_{o2}\tan^2(\theta_2) + z_{e2}\right]^2 + 4k^2\tan^2(\theta_2)z_{e2}z_{o2}} + \left[z_{o2}\tan^2(\theta_2) + z_{e2}\right]}{2k\tan(\theta_2)}} \\ z_{o1} &= \sqrt{\frac{\sqrt{\left[z_{o2}\tan^2(\theta_2) + z_{e2}\right]^2 + 4k^2\tan^2(\theta_2)z_{e2}z_{o2}} - \left[z_{o2}\tan^2(\theta_2) + z_{e2}\right]}{2k\tan(\theta_2)}} \end{aligned} \tag{13}$$

(16), the corresponding equations can be simplified as

$$\begin{cases} z_{o1} = \dfrac{1}{z_{e1}} \\ z_{e2} = \dfrac{k\left(z_{e1}^4-1\right)+\sqrt{k^2\left(z_{e1}^4-1\right)^2-4z_{e1}^4}}{2z_{e1}^2\cot(\theta_2)} \\ z_{o2} = \dfrac{k\left(z_{e1}^4-1\right)-\sqrt{k^2\left(z_{e1}^4-1\right)^2-4z_{e1}^4}}{2z_{e1}^2\tan\theta_2}. \end{cases} \tag{17}$$

It is very interesting that solution (17) is a special case of solution (12) when $z_{o1}z_{e1}=1$ is considered. However, it can be concluded that solution (12) cannot include totally solution (16), and vice versa. Therefore, two case discussions are necessary in theory.

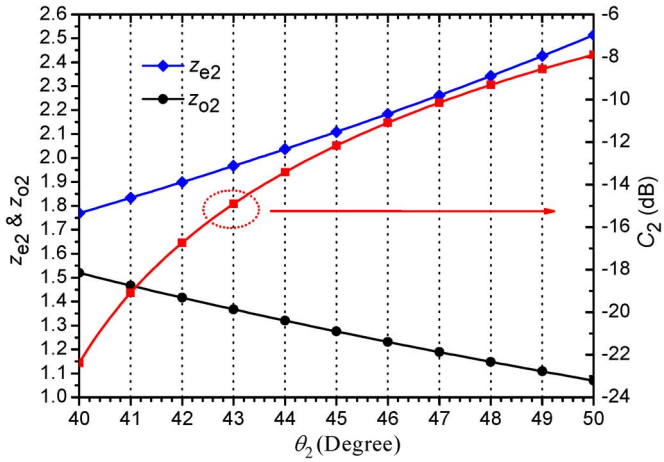


Fig. 3. Calculated design parameters and coupling coefficient of the proposed coupler with different electrical length $\theta_2$.

## III. Analysis of Circuit Electrical Parameters and Scattering Parameters

Based on the previous theoretical investigation, there are two different kinds of mathematical solutions (**Case 1 and Case 2**) for this novel coupled-line coupler. How to choose these two cases becomes a serious design problem. For the purpose of explanation, theoretical scattering parameters of typical examples designed using solution (12) or (16) are presented and discussed. For the convenience of discussion, the coupling coefficients of two-section coupled lines are defined as

$$C_i = \frac{z_{ei}-z_{oi}}{z_{ei}+z_{oi}}, \qquad i=1,2. \tag{18}$$

For the **Case 1** solution, the fixed circuit parameters of the following examples are $\theta_1=90^\circ$, $k=0.95$, $z_{e1}=2.05$, $z_{o1}=0.8$, $C_1=-7.16$ dB. For this given **tight coupling** requirement ($k=0.95<1$), other parameters such as $z_{e2}$ and $z_{o2}$ can be calculated by using (12) when the electrical length $\theta_2$ varies in the range of 40° to 50°. The calculated parameter curve is plotted in Fig. 3. It can be observed from Fig. 3 that the even-mode (odd-mode) characteristic impedance $z_{e2}$ ($z_{o2}$) shifts higher (lower) as the electrical length $\theta_2$ increases, indicating a strong coupling for the second section coupled line. The maximum coupling coefficient $C_2$ of the second coupled-line section is $-7.9$ dB, thus, two coupled lines have loose coupling. Therefore, two loosely coupled lines can be used to construct a coupler with external tight coupling performance. According to this numerical analysis, the admissible range of the coupling coefficient of the proposed coupler is $k\geq 0.95$. Although the 40° electrical length $\theta_2$ gives shorter physical length compared to the 50° electrical length $\theta_2$, the smaller coupling coefficient of the case $\theta_2=40^\circ$ results in a larger separation between coupled lines. Thus, there is a compromise between electrical length and coupling strength. To illustrate the theoretical response of the designed couplers in the normalized frequency band, two typical examples with $\theta_2=40^\circ$ and 50° are shown in Figs. 4 and 5, respectively. Good return loss, perfect isolation, precise phase difference, and almost $-3$-dB coupling can be observed clearly from both Figs. 4 and 5.

Next, if the electrical length $\theta_1$ is an arbitrary value in the range of (9b), but not equal to 90°, the design equation (16) should be chosen. In the **Case 2** solution, the following circuit parameters are fixed: $k=3$, $z_{e1}=1.4$, $\theta_2=40^\circ$. Another parameter $z_{o1}=0.7143$ can be obtained using (16). When the electrical length $\theta_1$ varies from 50° to 60°, the values of $z_{e2}$ and $z_{o2}$ with the corresponding coupling coefficient $C_2$ are as plotted in Fig. 6. Furthermore, the theoretical scattering parameters and phase difference of two typical examples as in Example A for $\theta_1=50^\circ$ and Example B for $\theta_1=60^\circ$ are illustrated in Fig. 7. Compared to the theoretical response of examples derived from the **Case 1** solution, the coupler designed

$$\begin{cases} z_{o1} = \dfrac{1}{z_{e1}} \\ z_{e2} = \dfrac{k\tan^2\theta_1\tan\theta_2\left(z_{e1}^4-1\right)+\tan\theta_2\sqrt{k^2\tan^4\theta_1\left(z_{e1}^4-1\right)^2-4z_{e1}^2\left[z_{e1}^2(1+\tan^2\theta_1)^2-k^2\tan^2\theta_1\left(z_{e1}^2-1\right)^2\right]}}{2z_{e1}\left[z_{e1}\left(1+\tan^2\theta_1\right)+k\tan\theta_1\left(z_{e1}^2-1\right)\right]} \\ z_{o2} = \dfrac{k\tan^2\theta_1\left(z_{e1}^4-1\right)-\sqrt{k^2\tan^4\theta_1\left(z_{e1}^4-1\right)^2-4z_{e1}^2\left[z_{e1}^2(1+\tan^2\theta_1)^2-k^2\tan^2\theta_1\left(z_{e1}^2-1\right)^2\right]}}{2z_{e1}\tan\theta_2\left[z_{e1}(1+\tan^2\theta_1)-k\tan\theta_1\left(z_{e1}^2-1\right)\right]} \end{cases} \tag{16}$$

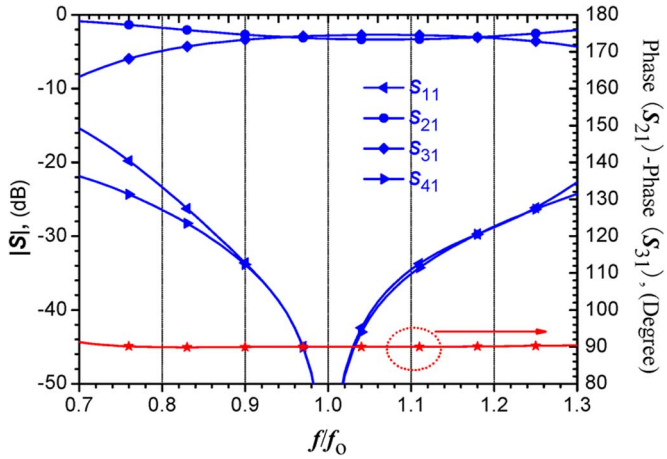


Fig. 4. Calculated scattering parameters and phase difference of the proposed coupler with electrical length $\theta_2 = 40°$.

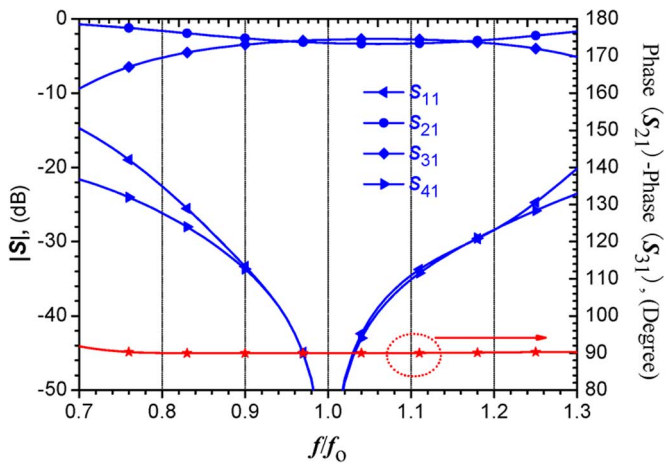


Fig. 5. Calculated scattering parameters and phase difference of the proposed coupler with electrical length $\theta_2 = 50°$.

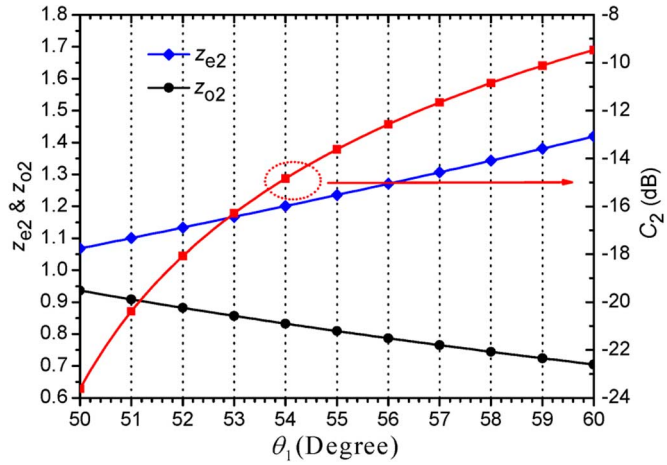


Fig. 6. Calculated design parameters and coupling coefficient of the proposed coupler with different electrical length $\theta_1$.

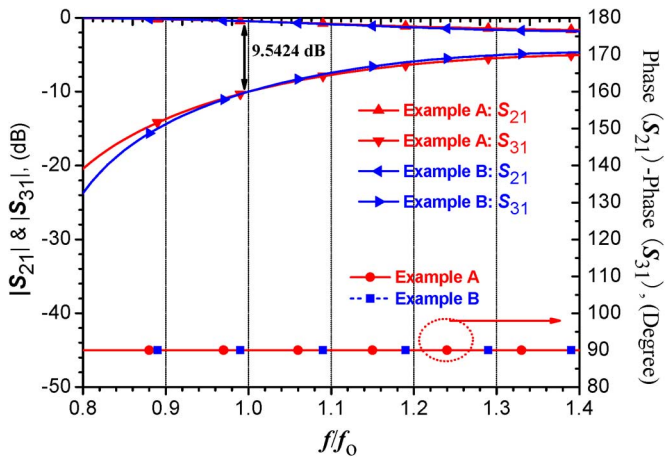


Fig. 7. Calculated scattering parameters and phase difference of the proposed couplers including Example A for $\theta_1 = 50°$ and Example B for $\theta_1 = 60°$.

using the **Case 2** solution (16) has two main differences, which are: 1) more suitable to design loose coupling performance such as $-10$ dB and 2) the response curve is usually not symmetrical, as shown in Fig. 7. As a result, because the tight coupling is required in this paper, only the **Case 1** solution is chosen in the following simulated and measured results. Since the analytical design and analysis equations are given, it is necessary to use effective optimization algorithms in looking for the most optimized solutions for different special requirement.

## IV. Full-Wave Simulated and Measured Results

The design theory and parameter analysis of this proposed coupled-line coupler has been theoretically explained in the aforementioned sections. However, the difference between the even- and odd-mode phase velocities are not considered in the analytical design equations such as in (12) and (16). Thus, the theoretically calculated scattering parameters in Figs. 4 and 5 are just used to illustrate the tight coupling performance without directivity deterioration. For demonstrative purposes, three full-wave simulated examples and a fabricated coupled-line coupler will be discussed in this section. These circuits or models are designed or fabricated using an RF substrate with a relatively dielectric constant of 2.65 and a thickness of 2 mm. These examples are designed using microstrip realization technology with a complete ground plane in the bottom layer. The operating frequency is chosen as 2 GHz. The above-layer circuit trace layout of the proposed coupler with defined dimension parameters is shown in Fig. 8.

According to design equation (12) based on previously manually chosen parameters such as electrical lengths and port impedance $Z_0 = 50\ \Omega$, the following initial practical electrical parameters are calculated and summarized as $\theta_1 = 90°$, $\theta_2 = 48°$, $k = 1$, $Z_{e1} = 100\ \Omega$, $Z_{o1} = 41\ \Omega$, $Z_{e2} = 107.9633\ \Omega$, and $Z_{o2} = 62.2804\ \Omega$. The initial physical circuit parameters are $w_1 = 2.66\ mm$, $s_1 = 0.17$ mm, $l_1 = 26$ mm, $w_2 = 2.05$ mm, $s_2 = 0.89$ mm, $l_2 = 14$ mm, and $w_m = 5.46$ mm. Note that the physical length $l_m$ of 50 $\Omega$ can be freely chosen according to practical design requirements. To accommodate the parasitic effects of junction discontinuity and the difference between the even- and odd-mode phase velocities, all simulated scattering parameters and phase information are finished with the help of the commercial electromagnetic full-wave simulation software Ansoft HFSS [24]. The maximum full-wave simulated directivity in the operating band

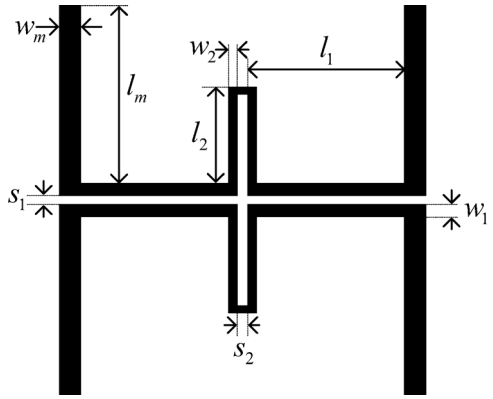


Fig. 8. Layout of the proposed tight-coupling high-directivity coupled-line coupler.

TABLE I
PHYSICAL CIRCUIT PARAMETERS (UNIT: MILLIMETERS) OF EXAMPLES 1–3

| Examples | $w_1$ | $w_2$ | $w_m$ | $s_1$ |
|---|---|---|---|---|
| **Example 1** | 2.8 | 1.8 | 5.5 | 0.4 |
| **Example 2** | 2.7 | 1.9 | 5.5 | 0.4 |
| **Example 3** | 2.5 | 2.2 | 5.5 | 0.2 |
| | $s_2$ | $l_1$ | $l_2$ | $l_m$ |
| **Example 1** | 1.0 | 25 | 14 | 20 |
| **Example 2** | 1.0 | 25 | 14 | 20 |
| **Example 3** | 0.4 | 25 | 15 | 20 |

(from 1 to 3 GHz) for the original coupled-line coupler without any optimizations is smaller than 30 dB. Since only four physical parameters, $w_1$, $w_2$, $s_1$, and $s_2$, are main optimized parameters, three examples, such as Examples 1–3, with high directivity can be easily achieved after simple manually optimizations. Their accurate physical circuit parameters are listed in Table I while the corresponding scattering parameters are plotted in Fig. 9. In Fig. 9, it can be observed that the highest directivity (almost 64.5 dB) occurs at the frequency 1.97 GHz in Example 2 while the strongest coupling (almost 1.6 dB) occurs at the frequency 2 GHz in Example 3 due to the smallest space separation in these three examples. Fortunately, these three examples achieve high directivity and strong coupling characteristics simultaneously.

Fig. 10 shows the fabricated microstrip coupled-line coupler. The physical circuit parameters are adopted from Example 1 due to the relatively large space separations $s_1 = 0.4$ mm and $s_2 = 1$ mm. Fig. 11 shows the measured scattering parameters and phase difference of the fabricated microstrip coupled-line coupler presented in Fig. 10. The measured results show that the return loss is better than 26.5 dB, coupling is larger than 5 dB, directivity is higher than 25 dB, and phase difference is near 90.5° ($\pm 0.6°$) over a wide range from 1.78 to 2 GHz. The measured directivity at 2 GHz is around 25 dB and the measured power division ratio $|S_{21}|/|S_{31}|$ at 2 GHz is smaller than 2 dB. The highest measured directivity is 36.6 dB at the frequency 1.88 GHz, while the strongest coupling is 4.22 dB at the frequency 2.04 GHz. Small frequency shifting and performance degradation could be due to the conductor loss, dielectric loss,

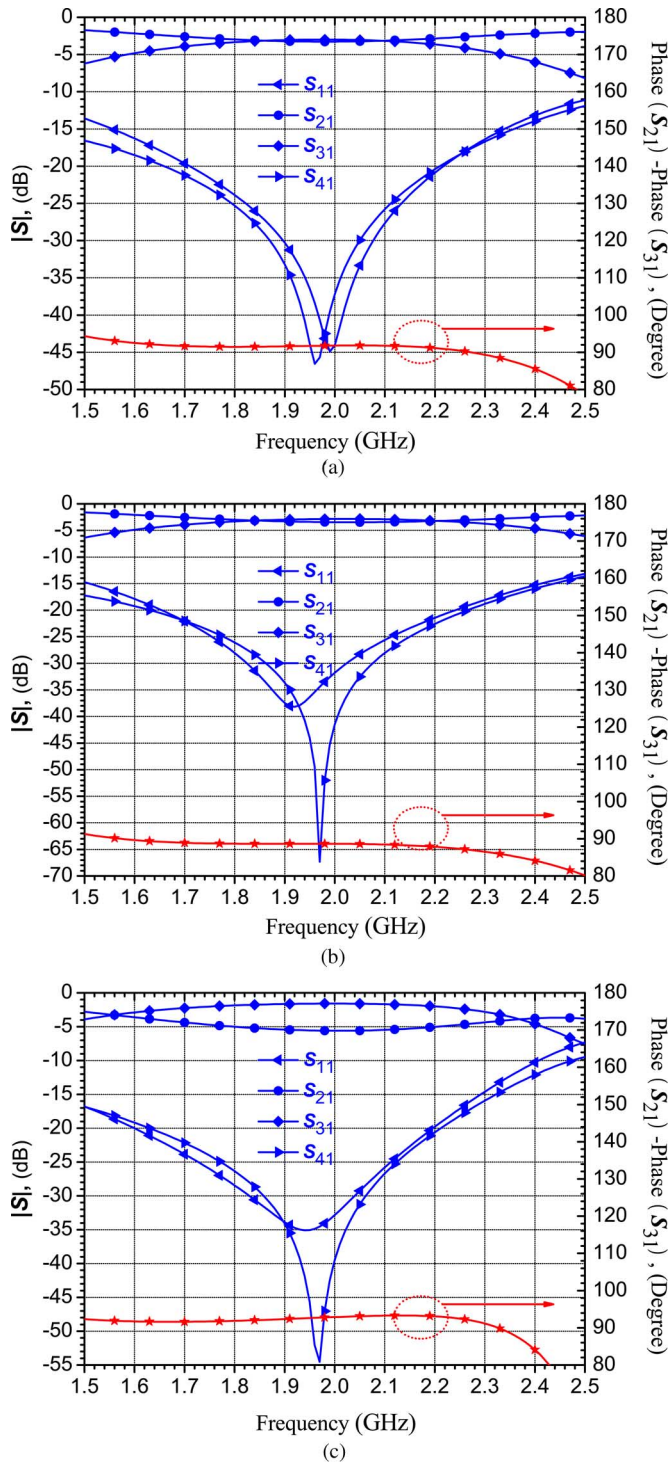


Fig. 9. Full-wave simulated scattering parameters and phase difference of: (a) Example 1, (b) Example 2, and (c) Example 3.

fabrication errors, or measurement errors. In general, the measured results of our proposed coupled-line coupler exhibit good return loss, strong coupling, and high directivity. It is very important that this coupler is implemented using common PCB fabrication technology without any limitations.

Based on the investigation on the proposed high-performance coupled-line coupler, a simple design procedure for this coupler can be summarized as follows.

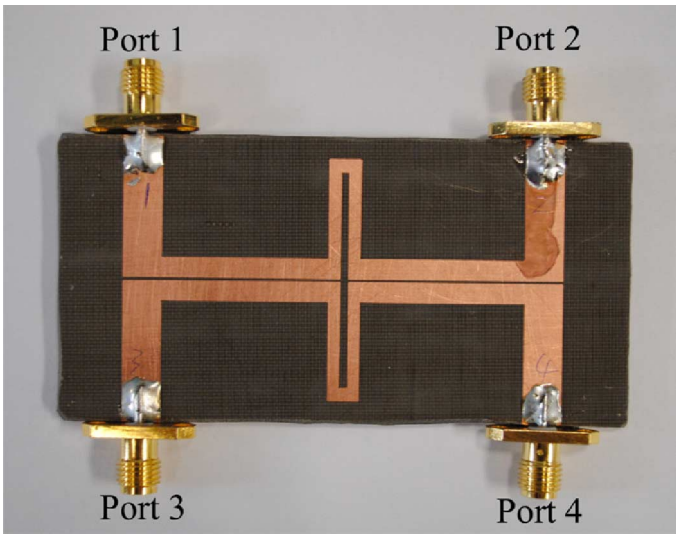


Fig. 10. Top view of the fabricated microstrip tight-coupling high-directivity coupled-line coupler.

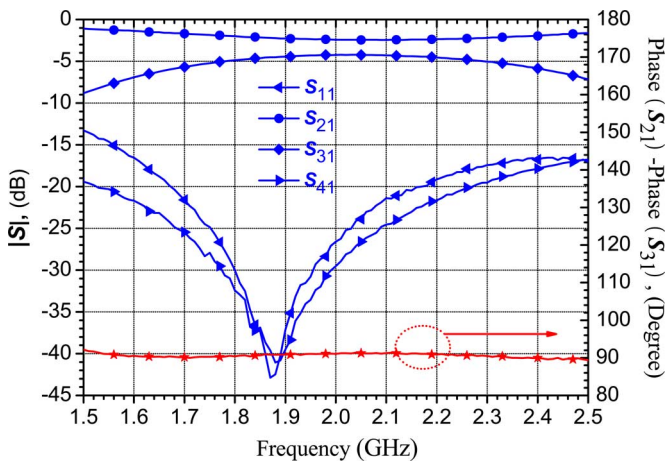


Fig. 11. Measured scattering parameters and phase difference of the fabricated tight-coupling high-directivity coupled-line coupler.

1) Determine the power-dividing coefficient $k$ and the center frequency $f_o$ according to the design requirements. Obtain the values of dielectric constant and thickness of the used substrate material.
2) Choose electrical length $\theta_2$, even (odd)-mode characteristic impedance $z_{e1}$ $(z_{o1})$. The values of $z_{e1}$ and $z_{o1}$ are mainly affected by the dielectric constant and thickness due to the minimum space limitation of the PCB etching process. Other electrical parameters of the proposed coupler are mainly calculated by these known coefficients in the above steps.
3) Calculate the even (odd)-mode characteristic impedance $z_{e2}$ $(z_{o2})$ by using the (12), and make sure that the coupling coefficient $C_2$ is calculated by (18) in the realized range.
4) Convert all the electrical parameters to the physical dimensions given in Fig. 8, and simulate the total scattering parameters and phase information by using full-wave simulation software tools such as HFSS and IE3D.
5) Tune the physical dimensions including $w_1$, $w_2$, $s_1$, and $s_2$ to obtain high directivity without affecting the coupling and matching performance. If the proper physical dimensions with the required performance cannot be achieved, the design should be restarted from (2) with other potential values.

## V. Conclusions

A novel coupled-line coupler has been proposed in this paper together with the design methodology and full-wave simulation verifications. This coupler, constructed by loose coupled lines, maintains strong coupling and high directivity simultaneously. To demonstrate the practical coupling and directivity performance, a microstrip coupled-line coupler is designed, fabricated, and measured. The measured return loss, coupling, and directivity are good, which verifies the proposed concept for high-performance couplers. Due to its simple circuit structure and ease of fabrication and integration in common microstrip systems, this proposed coupler is practical to use, especially in strong coupling situations.

## References

[1] R. Mongia, I. Bahl, and P. Bhartia, *RF and Microwave Coupled-Line Circuits*. Boston, MA: Artech House, 1999, pp. 1–21.
[2] S. Lee and Y. Lee, "An inductor-loaded microstrip directional coupler for directivity enhancement," *IEEE Microw. Wireless Compon. Lett.*, vol. 19, no. 6, pp. 362–364, Jun. 2009.
[3] J. Lange, "Interdigitated strip-line quadrature hybrid," *IEEE Trans. Microw. Theory Techn.*, vol. MTT-17, no. 12, pp. 1150–1151, Dec. 1969.
[4] J.-H. Cho, H.-Y. Hwang, and S.-W. Yun, "A design of wideband 3-dB coupler with $N$-section microstrip tandem structure," *IEEE Microw. Wireless Compon. Lett.*, vol. 15, no. 2, pp. 113–115, Feb. 2005.
[5] A. M. Abbosh and M. E. Bialkowski, "Design of compact directional couplers for UWB applications," *IEEE Trans. Microw. Theory Techn.*, vol. 55, no. 2, pp. 189–194, Feb. 2007.
[6] J.-C. Chiu, C.-M. Lin, and Y.-H. Wang, "A 3-dB quadrature coupler suitable for PCB circuit design," *IEEE Trans. Microw. Theory Techn.*, vol. 54, no. 9, pp. 3521–3525, Sep. 2006.
[7] J.-C. Chiu, J.-M. Lin, M.-P. Houng, and Y.-H. Wang, "A PCB-compatible 3-dB coupler using microstrip-to-CPW via-hole transitions," *IEEE Microw. Wireless Compon. Lett.*, vol. 16, no. 6, pp. 369–371, Jun. 2006.
[8] C.-P. Chang, J.-C. Chiu, H.-Y. Chiu, and Y.-H. Wang, "A 3-dB quadrature coupler using broadside-coupled coplanar waveguides," *IEEE Microw. Wireless Compon. Lett.*, vol. 18, no. 3, pp. 191–193, Mar. 2008.
[9] Y. X. Guo, Z. Y. Zhang, and L. C. Ong, "Wideband 3-dB coupler using a patterned ground plane," in *Proc. Asia–Pacific Microw. Conf.*, 2005, vol. 2.
[10] H.-C. Chen and C.-Y. Chang, "Modified vertically installed planar couplers for ultrabroadband multisection quadrature hybrid," *IEEE Microw. Wireless Compon. Lett.*, vol. 16, no. 8, pp. 446–448, Aug. 2006.
[11] T. Fujii, I. Ohta, T. Kawai, and Y. Kokubo, "A construction of coupled-line 3-dB couplers using quarter-wave connecting lines," in *Eur. Microw. Conf.*, 2005, vol. 1, pp. 37–40.
[12] Y.-H. Chun, J.-Y. Moon, S.-W. Yun, and J.-K. Rhee, "Microstrip line directional couplers with high directivity," *Electron. Lett.*, vol. 40, no. 5, pp. 317–318, Mar. 2004.
[13] K. Wincza and S. Gruszczynski, "Theoretical limits on miniaturization of directional couplers designed as a connection of tightly coupled and uncoupled lines," *Microw. Opt. Technol. Lett.*, vol. 55, no. 1, pp. 223–230, Jan. 2013.
[14] M.-J. Park and B. Lee, "Compact foldable coupled line cascade couplers," *Proc. Inst. Elect. Eng.—Microw., Antennas, Propag.*, vol. 153, no. 3, pp. 237–240, Jun. 2006.
[15] J. Muller and A. F. Jacob, "Advanced characterization and design of compensated high directivity quadrature coupler," in *IEEE MTT-S Int. Microw. Symp. Dig.*, 2010, pp. 724–727.
[16] M. Dydyk, "Microstrip directional couplers with ideal performance via single-element compensation," *IEEE Trans. Microw. Theory Techn.*, vol. 47, no. 6, pp. 956–964, Jun. 1999.
[17] S. Gruszczynski and K. Wincza, "Generalized methods for the design of quasi-ideal symmetric and asymmetric coupled-line sections and directional couplers," *IEEE Trans. Microw. Theory Techn.*, vol. 59, no. 7, pp. 1709–1718, Jul. 2011.

[18] I. Ohta, T. Kawai, T. Fujii, and Y. Kokubo, "Directivity improvement of microsrip coupled line couplers based on equivalent admittance approach," in *IEEE MTT-S Int. Microw. Symp. Dig.*, 2003, vol. 1, pp. 43–46.
[19] S.-F. Chang, J.-L. Chen, Y.-H. Jeng, and C.-T. Wu, "New high-directivity coupler design with coupled spurlines," *IEEE Microw. Wireless Compon. Lett.*, vol. 14, no. 2, pp. 65–67, Feb. 2004.
[20] R. Islam and G. V. Eleftheriades, "Printed high-directivity metamaterial MS/NRI coupled-line coupler for signal monitoring applications," *IEEE Microw. Wireless Compon. Lett.*, vol. 16, no. 4, pp. 164–166, Apr. 2006.
[21] X. Wang, W.-Y. Yin, and K.-L. Wu, "A dual-band coupled-line coupler with an arbitrary coupling coefficient," *IEEE Trans. Microw. Theory Techn.*, vol. 60, no. 4, pp. 945–951, Apr. 2012.
[22] J. Reed and G. J. Wheeler, "A method of analysis of symmetrical four port networks," *IRE Trans. Microw. Theory Techn.*, vol. MTT-4, no. 4, pp. 246–252, Oct. 1956.
[23] L. K. Yeung, "A compact dual-band 90 ° coupler with coupled-line sections," *IEEE Trans. Microw. Theory Techn.*, vol. 59, no. 9, pp. 2227–2232, Sep. 2011.
[24] High Frequency Structure Simulator (HFSS). ver. 13.0, ANSYS Inc., Canonsburg, PA, 2010.

**Yongle Wu** received the B. Eng. degree in communication engineering and Ph.D. degree in electronic engineering from the Beijing University of Posts and Telecommunications (BUPT), Beijing, China, in 2006 and 2011, respectively.

From April to October in 2010, he was a Research Assistant with the City University of Hong Kong (CityU), Kowloon, Hong Kong. In 2011, he joined the BUPT, and became a Lecturer with the School of Electronic Engineering. His research interests include generalized Smith charts, generalized transmission lines, and microwave components design.

**Weinong Sun** received the B.E. degree in communication engineering from Sun Yat-Sen University, Guangzhou, China, in 2010, and the Master's degree in electronic engineering from the City University of Hong Kong (CityU), Kowloon, Hong Kong, in 2012.

She is currently a Research Assistant with the Department of Electronic Engineering, CityU. Her research interests include electromagnetic field and microwave technology and human safety in electromagnetic compatibility.

**Sai-Wing Leung** (M'83–SM'03) was born in Hong Kong. He received the B.Sc. (Hons.) degree in electrical engineering and Ph.D. degree from City University, London, U.K., in 1976 and 1981, respectively.

In 1982, he joined the Engineering Division, ERA Technology Ltd., Leatherhead, U.K., as a Senior Engineer. In 1984, he joined the Hirst Research Centre, GEC Research Company Ltd., as a Principal Engineer, where he was responsible for leading a project on the development of electromagnetic launchers for armor-piercing applications. In 1985, he joined the Weapon Department, Thorn EMI Electronics Ltd., where he was responsible for the development of radar tracking of the multilaunch rocker system. In 1988, he joined the Martin Marietta Aerospace, Orlando, FL, where he was involved with the same system. Also in 1988, he joined the City University of Hong Kong (CityU), Kowloon, Hong Kong, as a Senior Lecturer. He is currently an Associate Professor with the Electronic Engineering Department and a Team Member of the Applied Electromagnetics Laboratory, CityU. He is actively involved in numerous consultancy projects assisting industry in both Hong Kong and overseas in solving electromagnetic compatibility/electromagnetic interference problems. He is the Director of the Electromagnetic Compatibility (EMC) Consulting Group, CityU Professional Services Ltd. He is an Assessor of the Hong Kong Laboratory Accreditation Scheme (HoKLAS) on the EMC area, and a member of the Working Party on Electrical and Electronic Products, Accreditation Advisory Board, Innovation and Technology Commission, Government of Hong Kong SAR.

Dr. Leung is the founding chairman of EMC Hong Kong Chapter, IEEE Hong Kong Section.

**Yinliang Diao** (S'12) received the B.E. degree from Chongqing University, Chongqing, China, in 2008, the Master's degree in electronic engineering from the Beijing University of Posts and Telecommunications, Beijing, China, in 2011, and is currently working toward the Ph.D. degree in electronic engineering at the City University of Hong Kong (CityU), Kowloon, Hong Kong.

His research interests include electromagnetic compatibility, electromagnetic field and microwave technology, and electromagnetic field simulation.

**Kwok-Hung Chan** (S'02–M'05) received the B.Eng. degree (with First Class Hons.) in electronic engineering and the M.Phil. and Ph.D. degrees from the City University of Hong Kong (CityU), Kowloon, Hong Kong, in 2001, 2004, and 2008, respectively.

In 2004, he was a Research Assistant with the Wireless Communications Research Centre, CityU. He is currently a Research Fellow with the Department of Electronic Engineering, CityU. His research interests include human safety and biomedical issues in electromagnetic compatibility, bioelectromagnetics, and electrostatic discharge.

Dr. Chan is the vice chairman of the IEEE Electromagnetic Compatibility Chapter, Hong Kong.

**Yun-Ming Siu** received the B.Sc. degree from the University of Manchester, Manchester, U.K., in 1981, and the Ph.D. degree from the University of Hong Kong, Kowloon, Hong Kong, in 1996.

From 1981 to 1989, he was with Racal-BCC U.K., initially as a Development Engineer and then a Principal Engineer responsible for the development of tactical communications systems. In 1990, he joined the City University of Hong Kong (CityU), Kowloon, Hong Kong, where he is currently an Associate Professor with the Department of Electronic Engineering. His current research interests include spread-spectrum techniques, electromagnetic compatibility, and information and communication networks.

Dr. Siu was the chairman of the Consumer Electronics Chapter, IEEE Hong Kong Section during 1998 and 1999.